Physica E 85 (2017) 271–279

Contents lists available at ScienceDirect

Physica E

journal homepage: www.elsevier.com/locate/physe

Different nano-particles volume fraction and Hartmann number effects on flow and heat transfer of water-silver nanofluid under the variable heat flux

Pezhman Forghani-Tehrani, Arash Karimipour*, Masoud Afrand, Sayedali Mousavi

Department of Mechanical Engineering, Najafabad Branch, Islamic Azad University, Najafabad, Iran

ARTICLE INFO

Keywords:
Magnetic field
Nano-particles
Hartmann number
Water-silver nanofluid

ABSTRACT

Nanofluid flow and heat transfer composed of water-silver nanoparticles is investigated numerically inside a microchannel. Finite volume approach (FVM) is applied and the effects of gravity are ignored. The whole length of Microchannel is considered in three sections as l_1=l_3=0.151 and l_2=0.71. The linear variable heat flux affects the microchannel wall in the length of l_2 while a magnetic field with strength of B_0 is considered over the whole domain of it. The influences of different values of Hartmann number (Ha=0, 10, 20), volume fraction of the nanoparticles (ϕ=0, 0.02, 0.04) and Reynolds number (Re=10, 50, 200) on the hydrodynamic and thermal properties of flow are reported. The investigation of slip velocity variations under the effects of a magnetic field are presented for the first time (to the best knowledge of author) while the non-dimensional slip coefficient are selected as B=0.01, 0.05, 0.1 at different states.

1. Introduction

Due to low thermal conductivity of simple pure fluids like water, many works have been reported in order to increase that thermal conductivity which led to generate a new composite called nanofluid which was a mixture of suspended nanoparticles in a liquid base fluid [1–6]. Several correlations have also been suggested to predict the nanofluid thermophysical properties; among them, Yu and Choi [7] have presented different models for its thermal conductivity. In the following, a large number of papers concerned nanofluid flow in enclosures and tubes can be addressed in this way [8–11].

The investigation of natural convection inside an enclosure filled with different types of nanofluid as like Cu-water, AL_2O_3-water and TiO_2-water was presented by Oztop and Abu-Nada [12] and the most value for Nusselt number was achieved for Cu-water. Moreover Jou and Tzeng [13] and Santra et al. [14] have studied other aspects of the nanofluid in rectangular cavities for example supposed it as the no-Newtonian liquid. Particle base methods like lattice Boltzmann approach can also be applied for the simulation of Cu-water nanofluid natural convection in an inclined lid driven cavity [15]. Many other works might be referred which concerned various types of nanofluid at different applications [16–20].

Simulation of flow and heat transfer through the microchannels has attracted several researchers recently. Due to small size and higher efficiency, that subject has being widely studied especially in the new industrials of MEMS and NEMS [21–24]. Tullius et al. [25] investigated the cooling process of the microchannel walls with various types of fluids and provided a desirable function about. Another interesting work involved nanofluid flow inside a microchannel was reported by Raisi et al. [26] who studied the effects of nanoparticles volume fraction and slip coefficient. Show the effects of gravity on a micro flow were also presented by Karimipour et al. [27] by lattice Boltzmann method. They proposed a range for Knudsen number to include the buoyance forces. More other studies can be addressed concerned the micro flows in this way [28–35].

It is possible to have the transverse magnetic field in several applications of devices; which strongly affects the hydrodynamic and thermal properties of domain. Back [36] investigated the flow and heat transfer between two parallel plates subjected to the electrical conductor. Show the influence of a magnetic field on the nanofluid flow through the microchannel was reported by Aminossadati et al. [37]. Simulations of MHD (magneto hydrodynamic) flows at different conditions are still continuing [38–45]. Also, several other new works can be referred concerned nanofluid flow which implies its novelty by now [50–55]; so that it is seen there is lack of researches concerned the magnetic field effect on nanofluid slip velocity which is presented here.

2. Problem statement

Nanofluid flow and heat transfer composed of water-silver nanoparticles is investigated numerically inside a microchannel. Fig. 1 illustrates the physical geometry of the microchannel with its aspect

* Corresponding author.
E-mail address: arashkarimipour@gmail.com (A. Karimipour).

http://dx.doi.org/10.1016/j.physe.2016.07.016
Received 23 May 2016; Received in revised form 20 June 2016; Accepted 12 July 2016
Available online 16 July 2016
1386-9477/

Nomenclature

B	Non-dimensional slip coefficient ($=\beta/h$)
B_0	The power of the magnetic field
Ha	Hartmann number ($=B_0 h\sqrt{\sigma_{nf}/\mu_{nf}}$)
Nu_x	Local Nusselt number
Nu_m	Averaged Nusselt number
q''_x	Heat flux, W/m^2
T_c	The temperature of the cold inlet nanofluid flow, K
u,v	velocity components, m/s
U,V	Non-dimensional velocity components
u_c	The velocity of inlet nanofluid flow, m/s
u_S	Slip velocity
U_S	Slip velocity in non-dimensional form
x,y	Cartesian coordinates, m
X,Y	Non-dimensional Cartesian coordinates

Greek symbols

ϕ	Volume fraction of nano particles
β	Slip coefficient, m
θ	Temperature in non-dimensional form
σ	Electrical conductivity, S/m

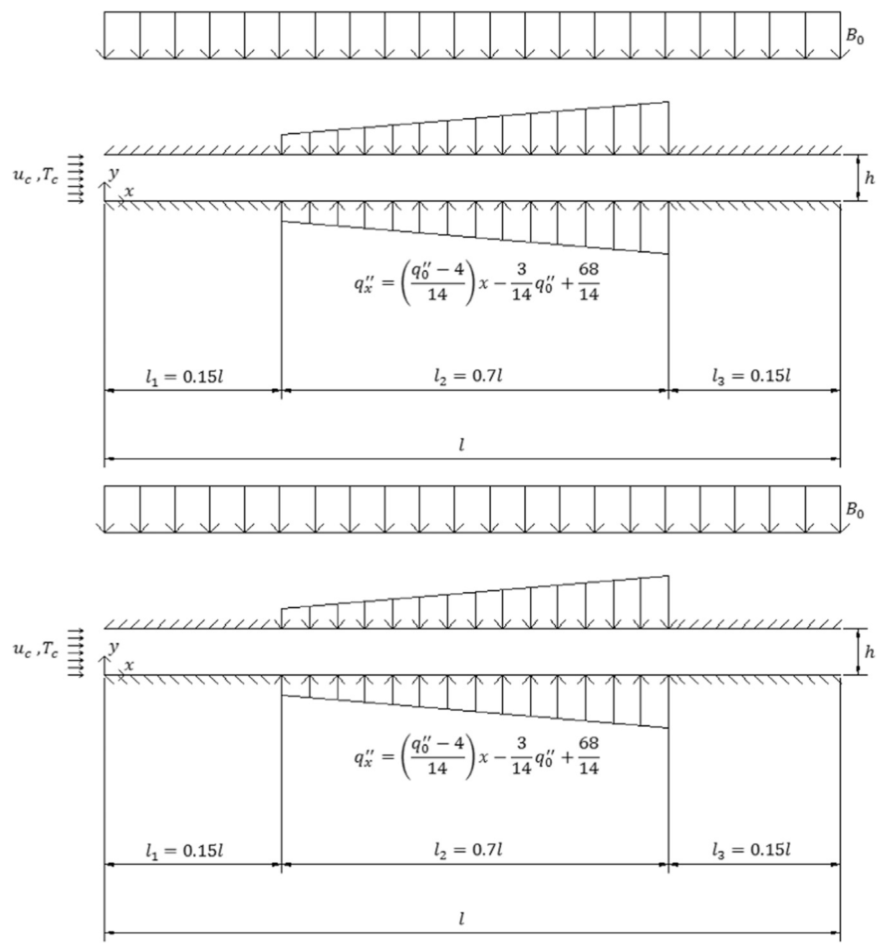

Fig. 1. The schematic physical domain of the microchannel.

Table 1
Thermo-physical properties of water (base fluid) and silver at 25 °C.

	μ	ρ	C_p	K
Pure water	0.8908×10^{-3}	997.1	4179	0.613
Ag nanoparticles		10,500	235	429

Table 2
Grid study at ϕ=0.04, Ha=10 and B=0.1.

Grids		400×20	600×30	800×40	1000×50
Re=10	Nu_m	4.060652	4.112199	4.140568	4.158858
	$\theta_{out,(Y=0.5)}$	0.747418	0.747433	0.74744	0.747443
	$U_{out,(Y=0.5)}$	1.1014	1.10263	1.10306	1.10326
Re=50	Nu_m	9.241925	9.415255	9.507361	9.565655
	$\theta_{out,(Y=0.5)}$	0.119025	0.118954	0.118921	0.118906
	$U_{out,(Y=0.5)}$	1.10138	1.10263	1.10306	1.10326

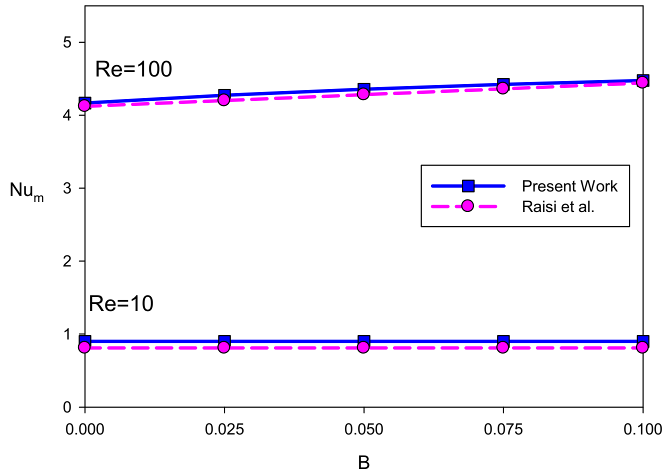

Fig. 2. Averaged Nusselt number in comparison with those of Raisi et al. [26] for ϕ=0.03.

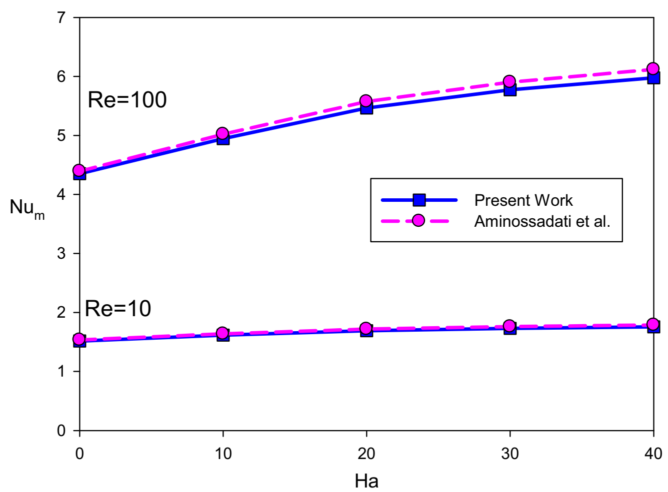

Fig. 3. Averaged Nusselt number in comparison with those of Aminossadati et al. [37] for ϕ=0.02.

ratio of $\frac{l}{h}$=20. The whole length of Microchannel is considered in three sections as l_1=l_3=0.151 and l_2=0.71. The linear variable heat flux affects the microchannel wall in the length of l_2 while a magnetic field with strength of B_0 is considered over the whole domain of it. The inlet cold Newtonian, incompressible nanofluid is supposed at T_c=293 °k. Moreover it is assumed that the silver spherical nanoparticles are at the same size with the diameter equal to d_p=10 nm.

Table 1 shows the thermo-physical properties of Ag nanoparticles and the water as the base fluid which implies that the Prandtl number of water would be 6.2. The influences of different values of Hartmann number (Ha=0, 10, 20), volume fraction of the nanoparticles (ϕ=0, 0.02, 0.04) and Reynolds number (Re=10, 50, 200) on the hydrodynamic and thermal properties of flow are reported. The investigation of slip velocity variations under the effects of a magnetic field are presented for the first time (to the best knowledge of author) while the non-dimensional slip coefficient are selected as B=0.01, 0.05, 0.1 at different states.

3. Numerical procedure and governing equations

The well-known Navier–Stokes equations are considered and solved numerically to simulate the supposed problem. However; the non-dimensional form of them can be achieved by the variables used in Eq. (1) for a 2-D domain under the effects of a magnetic field as follows:

$$X = \frac{x}{h}, Y = \frac{y}{h}, H = \frac{h}{h} = 1, L = \frac{l}{h} = 20, U = \frac{u}{u_c}, V = \frac{v}{u_c}, P = \frac{p}{\rho_{nf} u_c^2} \theta = \frac{T - T_c}{\Delta T}, \Delta T = \frac{q_0''}{k_{eff}}, \mathrm{Re} = \frac{\rho_{nf} u_c h}{\mu_{nf}}, \mathrm{Pr} = \frac{\upsilon_{nf}}{\alpha_{\mathrm{nf}}}, \mathrm{Ha} = B_0 h \sqrt{\sigma_{nf}/\mu_{nf}} \tag{1}$$

$$\frac{\partial U}{\partial X} + \frac{\partial V}{\partial Y} = 0 \tag{2}$$

$$U\frac{\partial U}{\partial X} + V\frac{\partial U}{\partial Y} = -\frac{\partial P}{\partial X} + \frac{1}{\mathrm{Re}}\left(\frac{\partial^2 U}{\partial X^2} + \frac{\partial^2 U}{\partial Y^2}\right) - \frac{Ha^2}{\mathrm{Re}}\mathrm{U} \tag{3}$$

$$U\frac{\partial V}{\partial X} + \mathrm{V}\frac{\partial V}{\partial Y} = -\frac{\partial P}{\partial Y} + \frac{1}{\mathrm{Re}}\left(\frac{\partial^2 V}{\partial X^2} + \frac{\partial^2 V}{\partial Y^2}\right) \tag{4}$$

$$U\frac{\partial \theta}{\partial X} + V\frac{\partial \theta}{\partial Y} = -\frac{\partial P}{\partial Y} + \frac{1}{\mathrm{RePr}}\left(\frac{\partial^2 \theta}{\partial X^2} + \frac{\partial^2 \theta}{\partial Y^2}\right) \tag{5}$$

It should be mentioned that nanofluid's properties are applied to determine the amounts of Re, Pr and Ha to have better agreements with the real physical problems. Moreover, the strength of magnetic field and electrical conductivity coefficient are shown by B_0 and σ_{nf}.

The nanofluid density is written as:

$$\rho_{nf} = \phi \rho_s + (1 - \phi)\rho_f \tag{6}$$

ϕ shows the volume fraction of nano particles; while n, f and s are related to the nanofluid, base fluid and solid nanoparticles, respectively.

The thermal diffusivity of nanofluid can be achieved as:

$$\alpha_{nf} = \frac{k_{eff}}{(\rho C_p)_{nf}} \tag{7}$$

Xuan and Li [46] formula is used to determine the nanofluid heat capacity:

$$(\rho C_p)_{nf} = (1 - \varphi)(\rho C_p)_f + \varphi(\rho C_p)_s \tag{8}$$

And finally the nanofluid viscosity is represented by Brinkman model as follows [47]:

$$\mu_{nf} = \frac{\mu_f}{(1 - \varphi)^{2.5}} \tag{9}$$

The model of Chon et al. [48] is used to calculate the nanofluid thermal conductivity. The resent model shows suitable accuracy and also the influences of Brownian motions and nanoparticles diameter can be considered in it.

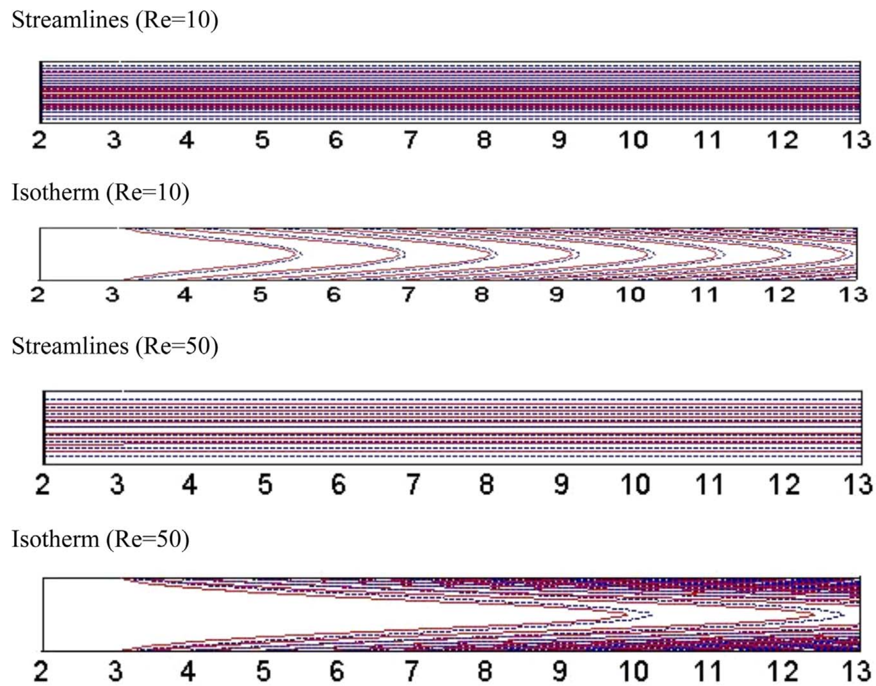

Fig. 4. Stream-lines and isotherm-contours at ϕ=0.04 and B=0.01 for Ha=0 (solid lines) and Ha=20 (dash lines).

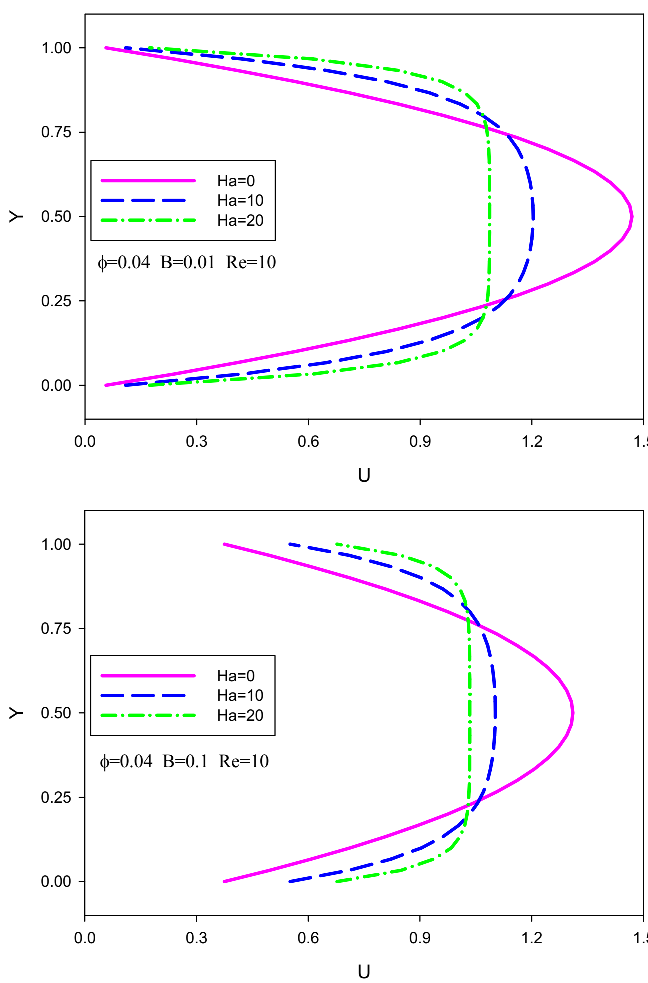

Fig. 5. U profiles on vertical centerline at ϕ=0.04, Re=10, B=0.01 and B=0.1.

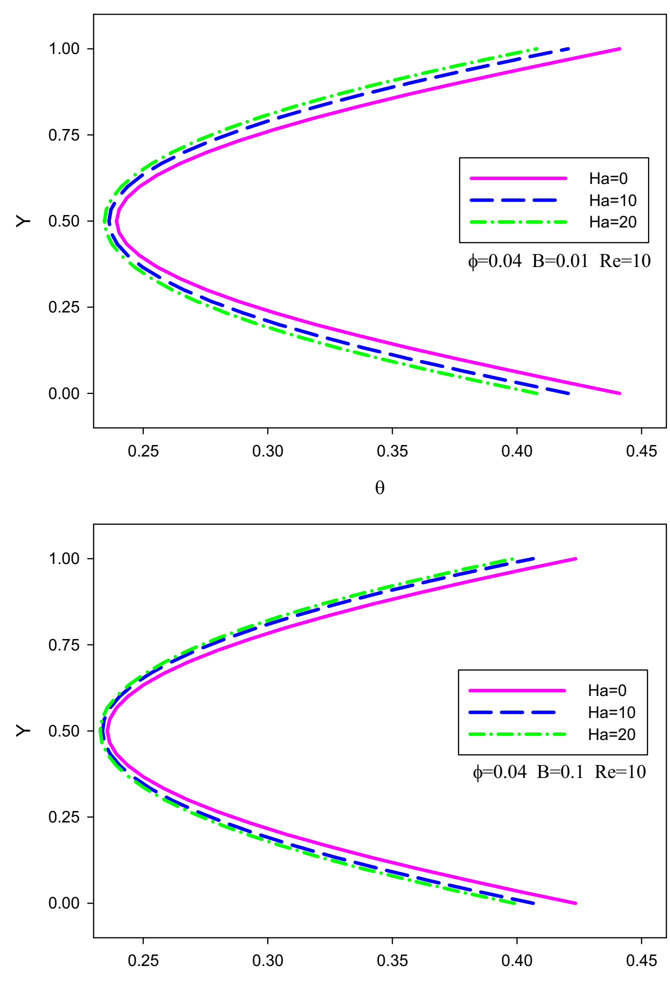

Fig. 6. θ profiles on vertical centerline at ϕ=0.04, Re=10, B=0.01 and B=0.1.

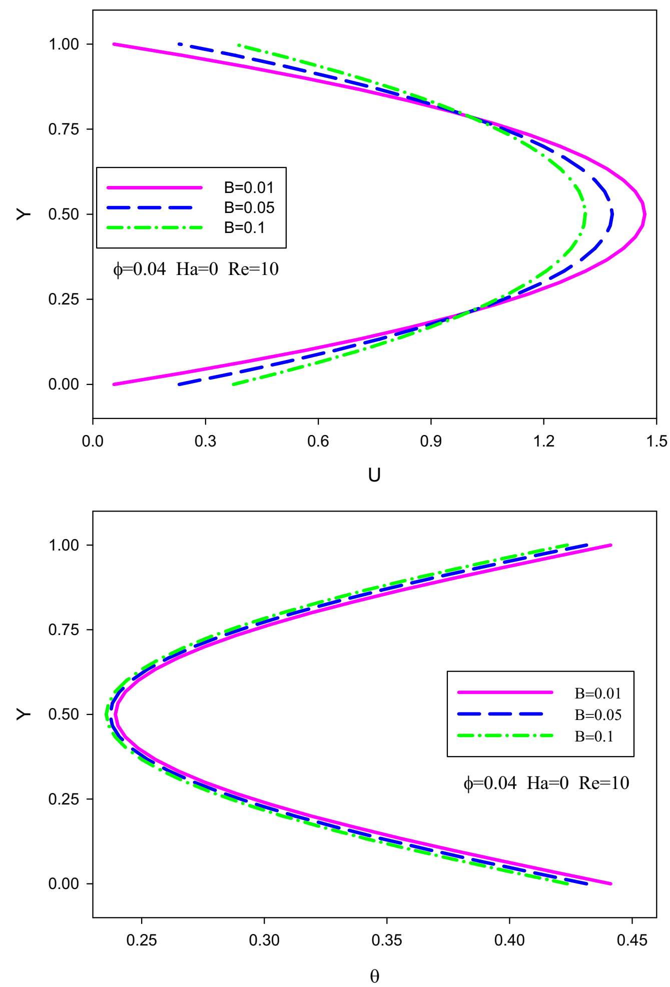

Fig. 7. U and θ profiles on vertical centerline at ϕ=0.04, Ha=0 and Re=10.

$$\frac{k_{nf}}{k_f}=1+64.\,7+\phi^{0.7460}+\left(\frac{d_f}{d_p}\right)^{0.3690}\left(\frac{k_s}{k_f}\right)^{0.7476}\left(\frac{\mu}{\rho_f\alpha_f}\right)^{0.9955}\left(\frac{\rho_f B_c T}{3\pi\mu^2 L_{BF}}\right)^{1.2321} \tag{10}$$

In Eq. (10), B_c=1.3807×10^{-23} and L_{BF} represent the Boltzmann coefficient and the mean free path of water molecules. It should be mentioned that diameter of water molecules are considered at d_f=0.17 nm while the amount of μ is determined as below at recent equation:

$$\mu = A10^{\frac{B}{T-C}},\ C=140(K),\ B=247(K),\ A=2.\,414\times10^{-5}\left(Pas\right) \tag{11}$$

As it is said before, the slip velocity boundary condition (u_s) is taken in to account at present study. To do this, the slip coefficient is shown by β [49]; hence u_s can be achieved along the microchannel walls as follows:

$$u_s=-\beta\left(\frac{\partial u}{\partial y}\right)_{y=h}\quad u_s=\beta\left(\frac{\partial u}{\partial y}\right)_{y=0} \tag{12}$$

The non-dimensional type of slip coefficient is introduced by $B=\frac{\beta}{h}$. As a result, all boundary conditions of the microchannel are shown in non-dimensional form as:

$$\begin{aligned}
&U=1,\ V=0\ \text{and}\ \theta=0\quad \text{for}\ X=0\ \text{and}\ 0\le Y\le 1\\
&V=0\ \text{and}\ \frac{\partial U}{\partial X}=\frac{\partial \theta}{\partial X}=0\quad \text{for}\ X=20\ \text{and}\ 0\le Y\le 1\\
&V=0,\ U_S=B\frac{\partial U}{\partial Y}\ \text{and}\ \frac{\partial \theta}{\partial Y}=0\ \text{or}\ \frac{\partial \theta}{\partial Y}=-\frac{1}{14}\left[\left(1-\frac{4}{q_0''}\right)(Xh)+\frac{68}{q_0''}-3\right]\text{for}\ Y=0\ \text{and}\ 0\le X\le 20\\
&V=0,\ U_S=-B\frac{\partial U}{\partial Y}\ \text{and}\ \frac{\partial \theta}{\partial Y}=0\ \text{or}\ \frac{\partial \theta}{\partial Y}=\frac{1}{14}\left[\left(1-\frac{4}{q_0''}\right)(Xh)+\frac{68}{q_0''}-3\right]\text{for}\ Y=1\ \text{and}\ 0\le X\le 20
\end{aligned} \tag{13}$$

In which U_S illustrates the non-dimensional form of slip velocity. Now, the Eqs. (2)–(5) are able to be solved numerically by finite volume method according to the SIMPLE algorithm.

Eqs. (14) and (15) are used for the local Nusselt number in dimensionless and dimensional forms, respectively:

$$(\mathrm{Nu}_x)_{y=0,h}=\frac{q_0''h}{(T_{S,x}-T_c)k_{nf}} \tag{14}$$

$$(\mathrm{Nu}_X)_{y=0,1}=\frac{1}{\theta_{S,X}} \tag{15}$$

Finally the averaged Nusselt number is determined as follows:

$$\mathrm{Nu}_m=\frac{1}{L_2}\int_{L_1}^{L_1+L_2}\mathrm{Nu}_X dX\qquad \left(L_1=\frac{l_1}{h}\ \text{and}\ L_2=\frac{l_2}{h}\right) \tag{16}$$

4. Grid independency and validations

Grid independency study is presented at different states in Table 2 for the amounts of the averaged Nusselt number and the outlet dimensionless velocity and temperature at Y=0.5, Re=50 and Re=10. As a result, the grid nodes of 800×40 are found suitable for the next computations. Moreover and for the validation; in Figs. 2 and 3 the values of Nusselt number along the microchannel walls are compared

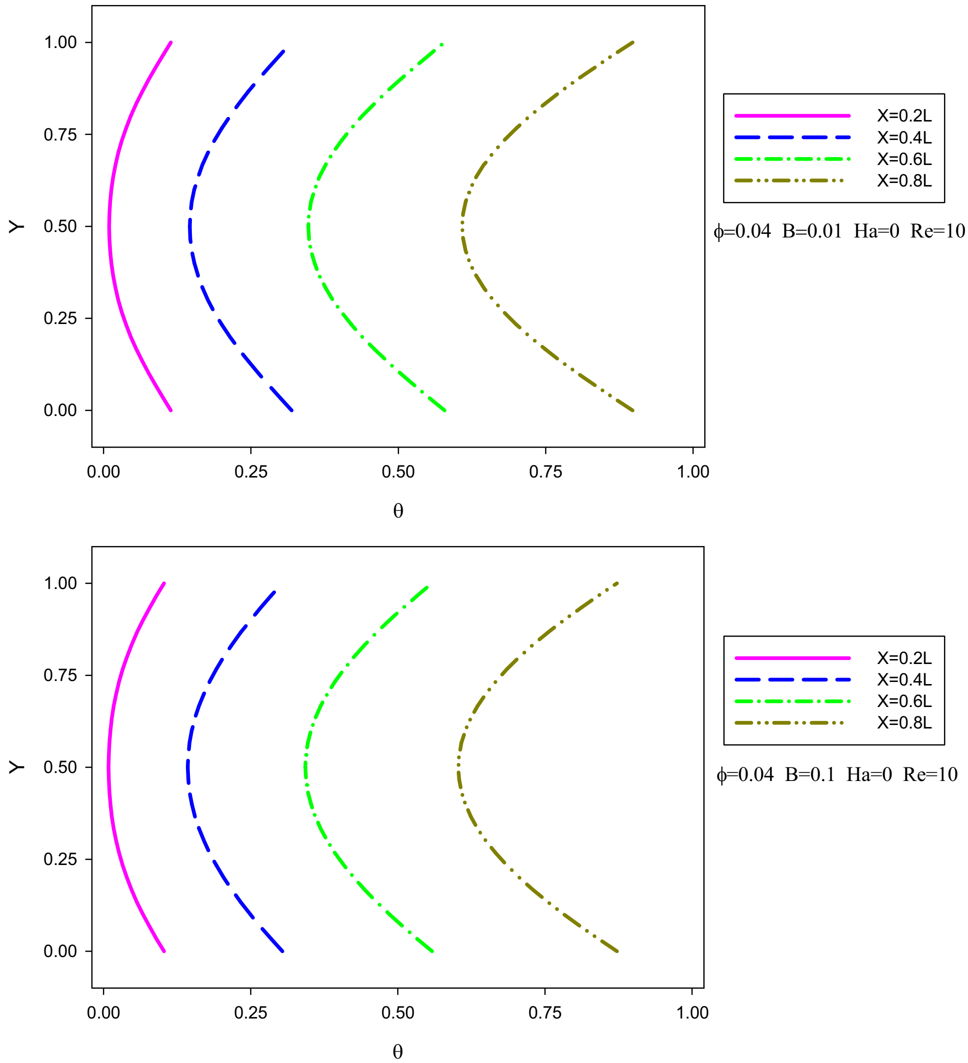

Fig. 8. θ profiles along the various cross-sections for ϕ=0.04, Ha=0 and Re=10.

with those of Raisi et al. [26] and Aminossadati et al. [37] respectively; and the suitable agreements are seen in these figures.

5. Results

The influences of various amounts of nanoparticles volume fractions, Hartmann number, slip coefficient and Reynolds number on the hydrodynamic and thermal properties of the water-Ag nanofluid inside a microchannel are simulated while the whole domain in under the uniform magnetic field. The following results are achieved.

5.1. Influences of Re and Ha

Fig. 4 illustrates the streamlines and isotherms for Ha=0, 20 and Re=10, 50 at ϕ=0.04 and B=0.01 which implies to the straight and parallel lines. Different values of Hartmann and Reynolds number don't significantly change these parallel streamlines. Although higher Re corresponds to higher entrance length. It is also seen that the isotherms intensity adjacent to the walls increases at larger amounts of Reynolds number.

In the following and in Fig. 5, the horizontal profiles of U on the microchannel vertical centerline are presented for Ha=0, 10, 20 and B=0.01, 0.1 at ϕ=0.04 and Re=10. The Lorentz force is generated in opposite direction of flow due to the existence of the magnetic field. Moreover U_{max} decreases by more Hartmann number which leads to higher values of U near the walls. This fact makes the change in the figure of fully developed velocity profiles from parabolic to the flat shape.

Dimensionless temperature profiles of θ on the vertical centerline at Ha=0, 10, 20 and B=0.01, 0.1 for ϕ=0.04 and Re=10 are presented through the Fig. 6. It is observed that cold nanofluid enters from the left side and then after passing the insulated section, it begins to be warmed under the effects of the heat flux along the length of L_2. That means the temperature of the nanofluid close the walls would be larger than the central areas. The less effects of Hartmann number on θ profiles can also be traced in this figure.

5.2. Influences of B and volume fraction

Fig. 7 presents U and θ profiles of nanofluid on the microchannel vertical centerline at B=0.01, B=0.05 and B=0.1 for Ha=0, Re=10 and ϕ=0.04. The amounts of U_s along the walls at B=0.01, B=0.05, B=0.1 are achieved as 0.056, 0.23, 0.374. Moreover the value of U_{max} decreases with B to satisfy the continuity equation. Although, θ profiles are not changed significantly by B. At present work, the temperature jump is ignored; As a result the slip coefficient only affects the hydrodynamic properties like slip velocity along the walls; so the temperature profiles would not significantly affected by B. In Fig. 8, the profiles of θ at various cross-sections are observed at B=0.1, B=0.01 and for ϕ=0.4, Re=10, Ha=0. Due to imposed heat flux over the

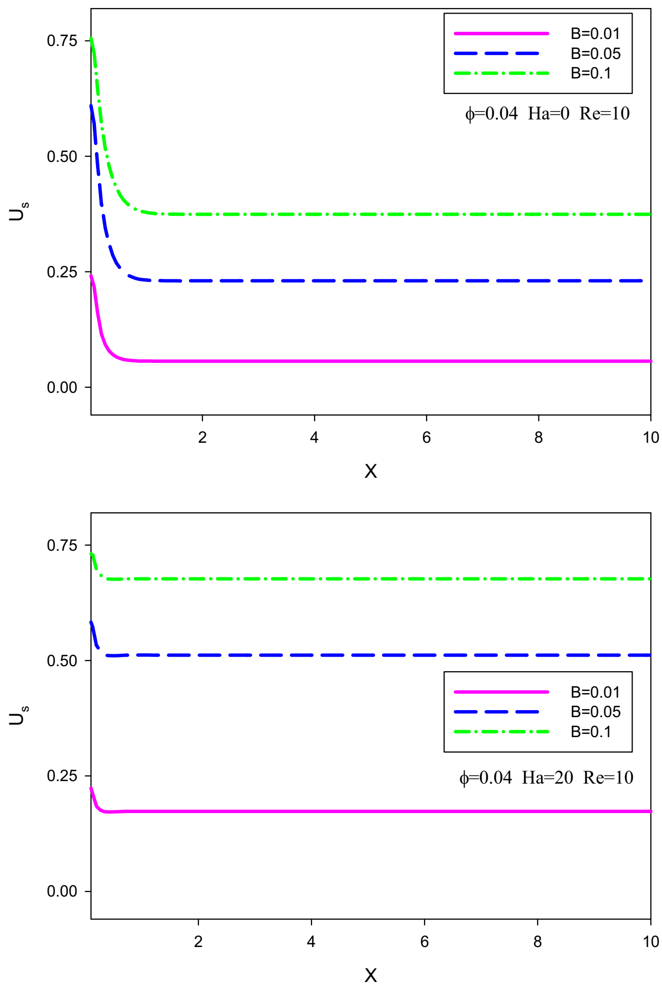

Fig. 9. U_s on the wall of microchannel for ng the microchannel for ϕ=0.04, Re=10, Ha=0 and Ha=20.

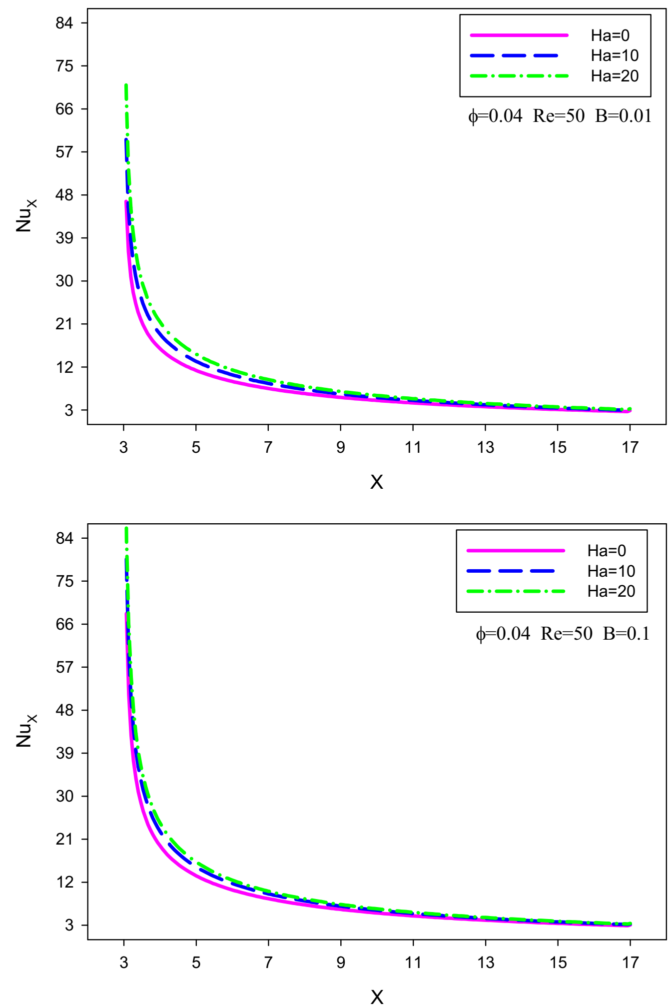

Fig. 10. Nu_X on the wall of microchannel for ϕ=0.04, Re=50, B=0.01 and B=0.1.

microchannel walls, the temperature of nanofluid increases with X. Change the curve figure of temperature profiles from the flat shape at X=0.2 L to the parabolic one at X=0.8 L can be observed clearly in this figure; that event has not been reported in previous articles.

Fig. 9 illustrates the U_s along the microchannel walls at B=0.01, 0.05, 0.1 and for ϕ=0.04, Re=10. Slip velocity has maximum value at inlet and it starts to decrease with X, so that it tends to the constant amount. More U_s is achieved by more slip coefficient; although this event is happened more severely at larger Hartmann number.

Local Nusselt number on the walls at various amounts of Hartmann number and slip coefficient for ϕ=0.04 and Re=50 are presented through the Fig. 10. Obviously, Nusselt number equals to zero through the adiabatic sections and then its maximum amount can be found at X=3. More X corresponds to less Nu_X until X=17 where is the start point of second insulated area.

At last, the values of Nu_m on the length of L_2 are shown in Fig. 11 for various amounts of Reynolds number, Hartmann number, slip coefficient and nanoparticles volume fraction. At the state of Re=10, the averaged Nusselt number decreases while volume fraction changes from ϕ=0.02 to ϕ=0.04. This fact is seen for the first time at present work. However higher Reynolds number corresponds to change in this manner so that at Re=200, more Nusselt number is observed for larger amount of volume fraction. It should be mentioned that the values of nanofluid Reynolds number through the microchannel are usually small; hence applying nanofluid with more volume fraction to increase Nusselt number would not be so desirable action. Although this deficiency might be improved by the influences of the slip coefficient and the stronger magnetic field.

6. Conclusion

Nanofluid flow and heat transfer composed of water-silver nanoparticles was investigated numerically inside a microchannel. Finite volume approach (FVM) was applied and the effects of gravity were ignored. The whole length of Microchannel was considered in three sections as l_1=l_3=0.151 and l_2=0.71. The linear variable heat flux affected the microchannel wall in the length of l_2 while a magnetic field with strength of B_0 was considered over the whole domain of it. The influences of different values of Hartmann number (Ha=0, 10, 20), volume fraction of the nanoparticles (ϕ=0, 0.02, 0.04) and Reynolds number (Re=10, 50, 200) on the hydrodynamic and thermal properties of flow were reported. The investigation of slip velocity variations under the effects of a magnetic field were presented for the first time (to the best knowledge of author) while the non-dimensional slip coefficients were selected as B=0.01, 0.05, 0.1 at different states.

The Lorentz force was generated due to the magnetic field existence in the opposite direction of flow. This fact corresponded to less the maximum value of horizontal velocity and more velocity adjacent to the walls. Larger slip coefficient led to more U_s especially at higher amounts of Hartmann number. The recent event was reported for the first time at present article and has not been seen in previous ones; hence the detour from continuous regime might be observed sooner at higher strength of the magnetic field.

Increasing ϕ from ϕ=0.02 to ϕ=0.04 at Re=10 generated lower

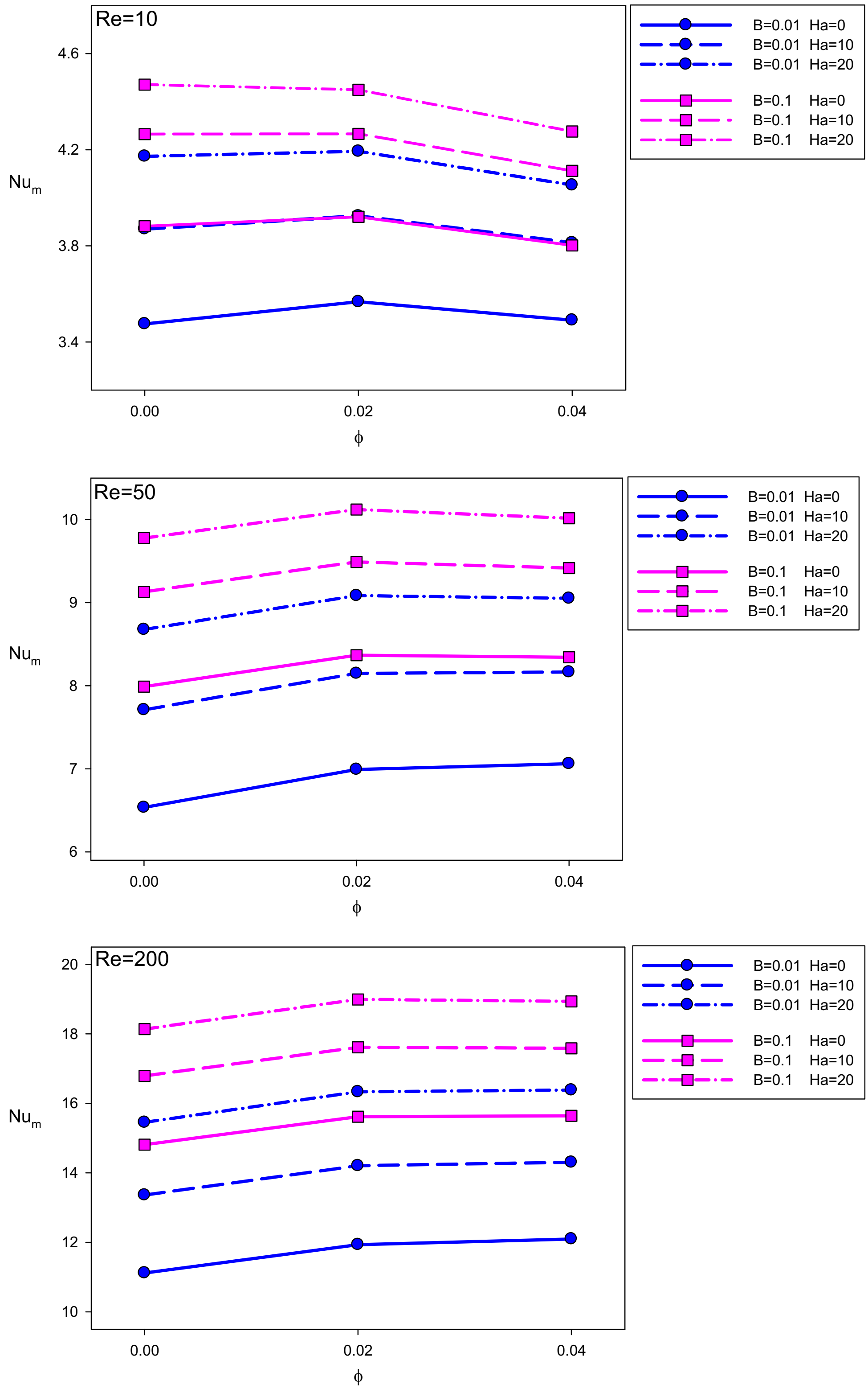

Fig. 11. Averaged Nusselt number on the wall of microchannel for various amounts of ϕ, Ha, Re and B.

Nu$_m$; however at Re=200 higher Nusselt number was observed at more volume fraction. It should be mentioned that the Reynolds number of nanofluids inside the microchannels usually had the small amounts; hence using more volume fraction to increase Nu would not be so desirable at micro and nano flows. Although, this fact might be improved by the magnetic field and slip coefficient influences.

References

[1] S. Lee, S.U.S. Choi, S. Li, J.A. Eastman, Measuring thermal conductivity of fluids containing oxide nanoparticles, ASME J. Heat. Transf. 121 (1999) 280–289.

[2] M.H. Esfe, M. Akbari, D. Toghraie, A. Karimipour, M. Afrand, Effect of nanofluid variable properties on mixed convection flow and heat transfer in an inclined two-sided lid-driven cavity with sinusoidal heating on sidewalls, Heat. Transf. Res. 45 (2014) 409–432.

[3] A. Karimipour, New correlation for Nusselt number of nanofluid with Ag/Al$_2$O$_3$/Cu

nanoparticles in a microchannel considering slip velocity and temperature jump by using lattice Boltzmann method, Int. J. Therm. Sci. 91 (2015) 146–156.
[4] M. Goodarzi, M.R. Safaei, A. Karimipour, K. Hooman, M. Dahari, S.N. Kazi, E. Sadeghinezhad, Comparison of the Finite Volume and Lattice Boltzmann Methods for Solving Natural Convection Heat Transfer Problems Inside Cavities and Enclosures, Abstract and Applied Analysis, Vol. 2014, Hindawi Publishing Corporation, 2014 February.
[5] M.H. Esfe, A.A.A. Arani, A. Karimipour, S.S.M. Esforjani, Numerical simulation of natural convection around an obstacle placed in an enclosure filled with different types of nanofluids, Heat. Transf. Res. 45 (3) (2014) 279–292.
[6] A. Karimipour, A.H. Nezhad, A. D'Orazio, E. Shirani, The effects of inclination angle and Prandtl number on the mixed convection in the inclined lid driven cavity using lattice Boltzmann method, J. Theor. Appl. Mech. 51 (2) (2013) 447–462.
[7] W. Yu, S.U.S. Choi, The role of interfacial layers in the enhanced thermal conductivity of nanofluids: a renovated Maxwell model, J. Nanopart. Res. 5 (2003) 167–171.
[8] A. Malvandi, Ghasemi Amirmahdi, D.D. Ganji, Thermal performance analysis of hydromagnetic Al_2O_3-water nanofluid flows inside a concentric microannulus considering nanoparticle migration and asymmetric heating, Int. J. Therm. Sci. 109 (2016) 10–22.
[9] A. Karimipour, A.H. Nezhad, A. D'Orazio, M.H. Esfe, M.R. Safaei, E. Shirani, Simulation of copper–water nanofluid in a microchannel in slip flow regime using the lattice Boltzmann method, Eur. J. Mech.-B/Fluids 49 (2015) 89–99.
[10] A. Karimipour, A.H. Nezhad, A. Behzadmehr, S. Alikhani, E. Abedini, Periodic mixed convection of a nanofluid in a cavity with top lid sinusoidal motion, Proc. Inst. Mech. Eng. Part C: J. Mech. Eng. Sci. 225 (2011) 2149–2160.
[11] Z. Nikkhah, A. Karimipour, M.R. Safaei, P. Forghani-Tehrani, M. Goodarzi, M. Dahari, S. Wongwises, Forced convective heat transfer of water/functionalized multi-walled carbon nanotube nanofluids in a microchannel with oscillating heat flux and slip boundary condition, Int. Commun. Heat Mass Transf. 68 (2015) 69–77.
[12] H.F. Oztop, E. Abu-Nada, Numerical study of natural convection in partially heated rectangular enclosures filled with nanofluids, Int. J. Heat. Fluid Flow 29 (2008) 1326–1336.
[13] R.Y. Jou, S.C. Tzeng, Numerical research of natural convective heat transfer enhancement filled with nanofluids in rectangular enclosures, Int. Commun. Heat Mass Transf. 33 (2006) 727–736.
[14] A.K. Santra, S. Sen, N. Chakraborty, Study of heat transfer due to laminar flow of copper-water nanofluid through two isothermally heated parallel plates, Int. J. Therm. Sci. 48 (2009) 391–400.
[15] A. Karimipour, M.H. Esfe, M.R. Safaei, D.T. Semiromi, S.N. Kazi, Mixed convection of copper–water nanofluid in a shallow inclined lid driven cavity using the lattice Boltzmann method, Physica A 402 (2014) 150–168.
[16] A. Malvandi, S. Heysiattalab, D.D. Ganji, Thermophoresis and Brownian motion effects on heat transfer enhancement at film boiling of nanofluids over a vertical cylinder, J. Mol. Liq. 216 (2016) 503–509.
[17] M.H. Esfe, A.A.A. Arani, M. Rezaie, W.M. Yan, A. Karimipour, Experimental determination of thermal conductivity and dynamic viscosity of Ag–MgO/water hybrid nanofluid, Int. Commun. Heat Mass Transf. 66 (2015) 189–195.
[18] M.H. Esfe, A. Karimipour, W.M. Yan, M. Akbari, M.R. Safaei, M. Dahari, Experimental study on thermal conductivity of ethylene glycol based nanofluids containing Al_2O_3 nanoparticles, Int. J. Heat Mass Transf. 88 (2015) 728–734.
[19] M.H. Esfe, M. Akbari, A. Karimipour, M. Afrand, O. Mahian, S. Wongwises, Mixed-convection flow and heat transfer in an inclined cavity equipped to a hot obstacle using nanofluids considering temperature-dependent properties, Int. J. Heat Mass Transf. 85 (2015) 656–666.
[20] M.H. Esfe, A. Naderi, M. Akbari, M. Afrand, A. Karimipour, Evaluation of thermal conductivity of COOH-functionalized MWCNTs/water via temperature and solid volume fraction by using experimental data and ANN methods, J. Therm. Anal. Calorim. 121 (3) (2015) 1273–1278.
[21] O. Mokrani, B. Bourouga, C. Castelain, H. Peerhossaini, Fluid flow and convective heat transfer in flat microchannels, Int. J. Heat Mass Transf. 52 (2009) 1337–1352.
[22] A. Malvandi, D.D. Ganji, Brownian motion and thermophoresis effects on slip flow of alumina/water nanofluid inside a circular microchannel in the presence of a magnetic field, Int. J. Therm. Sci. 84 (2014) 196–206.
[23] A. Malvandi, D.D. Ganji, Effects of nanoparticle migration and asymmetric heating on magnetohydrodynamic forced convection of alumina/water nanofluid in microchannels, Eur. J. Mech.-B/Fluids *52* (2015) 169–184.
[24] D.B. Tuckerman, R.F.W. Pease, High-performance heat sinking for VLSI, IEEE Electron Device Lett. 2 (1981) 126–129.
[25] J.F. Tullius, R. Vajtai, Y. Bayazitoglu, A review of cooling in microchannels, Heat Transf. Eng. 32 (2011) 527–541.
[26] A. Raisi, B. Ghasemi, S.M. Aminossadati, A numerical study on the forced convection of laminar nanofluid in a microchannel with both slip and no-slip conditions, Numer. Heat Transf.; Part A 59 (2011) 114–129.
[27] A. Karimipour, A.H. Nezhad, A. D'Orazio, E. Shirani, Investigation of the gravity effects on the mixed convection heat transferin a microchannel using lattice Boltzmann method, Int. J. Therm. Sci. 54 (2012) 142–152.
[28] Z. Duan, Y.S. Muzychka, Slip flow in elliptic microchannels, Int. J. Therm. Sci. 46 (2007) 1104–1111.
[29] A. Akbarinia, M. Abdolzadeh, R. Laur, Critical investigation of heat transfer enhancement using nanofluids in microchannels with slip and non-slip flow regimes, Appl. Therm. Eng. 31 (2011) 556–565.
[30] K. Anoop, R. Sadr, J. Yu, S. Kang, S. Jeon, D. Banerjee, Experimental study of forced convective heat transfer of nanofluids in a microchannel, Int. Commun. Heat Mass Transf. 39 (2012) 1325–1330.
[31] J.Y. Jung, H.S. Oh, H.Y. Kwak, Forced convective heat transfer of nanofluids in microchannels, Int. J. Heat Mass Transf. 52 (2009) 466–472.
[32] J. Lee, I. Mudawar, Assessment of the effectiveness of nanofluids for single phase and two-phase heat transfer in micro-channels, Int. J. Heat Mass Transf. 50 (2007) 452–463.
[33] P. Rosa, T.G. Karayiannis, M.W. Collins, Single-phase heat transfer in micro-channels: the importance of scaling effects, Appl. Therm. Eng. 29 (2009) 3447–3468.
[34] J. Li, C. Kleinstreuer, Thermal performance of nanofluid flow in microchannels, Int. J. Heat Fluid Flow 29 (2008) 1221–1232.
[35] B. Buonomo, O. Manca, Transient natural convection in a vertical microchannel heated at uniform heat flux, Int. J. Therm. Sci. 56 (2012) 35–47.
[36] L.H. Back, Laminar heat transfer in electrically conducting fluids flowing in parallel plate channels, Int. J. Heat Mass Transf. 11 (1968) 1621–1636.
[37] S.M. Aminossadati, A. Raisi, B. Ghasemi, Effects of magnetic field on nanofluid forced convection in a partially heated microchannel, Int. J. Non-Linear Mech. 46 (2011) 1373–1382.
[38] R.U. Haq, S. Nadeem, Z.H. Khan, N.S. Akbar, Thermal radiation and slip effects on MHD stagnation point flow of nanofluid over a stretching sheet, Phys. E: Low-Dimens. Syst. Nanostruct. *65* (2015) 17–23.
[39] N.S. Akbar, Ferromagnetic CNT suspended H_2O+Cu nanofluid analysis through composite stenosed arteries with permeable wall, Phys. E: Lo.-Dimens. Syst. Nanostruct. *72* (2015) 70–76.
[40] J.A. Lima, J.N.N. Queresma, E.N. Macedo, Integral transform analysis of MHD flow and heat transfer in parallel-plates channels, Int. Commun. Heat Mass Transf. 34 (2007) 420–431.
[41] M.A.A. Hamad, Analytical solution of natural convection flow of a nanofluid over a linearly stretching sheet in the presence of magnetic field, Int. Commun. Heat Mass Transf. 38 (2011) 487–492.
[42] A.H. Mahmoudi, I. Pop, M. Shahi, Effect of magnetic field on natural convection in a triangular enclosure filled with nanofluid, Int. J. Therm. Sci. 59 (2012) 126–140.
[43] B. Ghasemi, S.M. Aminossadati, A. Raisi, Magnetic field effect on natural convection in a nanofluid-filled square enclosure, Int. J. Therm. Sci. 50 (2011) 1748–1756.
[44] M.A.A. Hamad, I. Pop, A.I.Md Ismail, Magnetic field effects on free convection flow of a nanofluid past a vertical semi-infinite flat plate, J. Nonlinear Anal.: Real World Appl. 12 (2011) 1338–1346.
[45] M. Sheikholeslami, M. Gorji-Bandpay, D.D. Ganji, Magnetic field effects on natural convection around a horizontal circular cylinder inside a square enclosure filled with nanofluid, Int. Commun. Heat Mass Transf. 39 (2012) 978–986.
[46] Y. Xuan, Q. Li, Investigation on convective heat transfer and flow features of nanofluids, ASME. J. Heat Transf. 125 (2003) 151–155.
[47] H.C. Brinkman, The viscosity of concentrated suspensions and solution, J. Chem. Phys. 20 (1952) 571–581.
[48] C.H. Chon, K.D. Kihm, S.P. Lee, S.U.S. Choi, Empirical correlation finding the role of temperature and particle size for nanofluid (AL_2O_3) thermal conductivity enhancement, Appl. Phys. Lett. 87 (2005) 1–3.
[49] G.D. Ngoma, F. Erchiqui, Heat flux and slip effects on liquid flow in a micro-channel, Int. J. Therm. Sci. 46 (2007) 1076–1083.
[50] A. Malvandi, D.D. Ganji, Effects of nanoparticle migration on hydromagnetic mixed convection of alumina/water nanofluid in vertical channels with asymmetric heating, Phys. E: Low-Dimens. Syst. Nanostruct. 66 (2015) 181–196.
[51] A. Malvandi, S.A. Moshizi, D.D. Ganji, Two-component heterogeneous mixed convection of alumina/water nanofluid in microchannels with heat source/sink, Adv. Powder Technol. 27 (1) (2016) 245–254.
[52] S. Shamshirband, A. Malvandi, A. Karimipour, M. Goodarzi, M. Afrand, D. Petković, M. Dahari, N. Mahmoodian, Performance investigation of micro-and nano-sized particle erosion in a 90 elbow using an ANFIS model, Powder Technol. 284 (2015) 336–343.
[53] A. Malvandi, Film boiling of magnetic nanofluids (MNFs) over a vertical plate in presence of a uniform variable-directional magnetic field, J. Magn. Magn. Mater. 406 (2016) 95–102.
[54] M.A. Sheremet, S. Dinarvand, I. Pop, Effect of thermal stratification on free convection in a square porous cavity filled with a nanofluid using Tiwari and Das' nanofluid model, Phys. E: Low.-Dimens. Syst. Nanostruct. *69* (2015) 332–341.
[55] F.M. Abbasi, T. Hayat, B. Ahmad, Peristaltic transport of copper–water nanofluid saturating porous medium, Physica E: Low-Dimens. Syst. Nanostruct. *67* (2015) 47–53.